Hybridization and transgressive exploration of colour pattern and wing morphology in Heliconius butterflies

Claire Mérot, Vincent Debat, Yann Le Poul, Richard Merrill, Russell Naisbit, Adélie Tholance, Chris Jiggins, Mathieu Joron

JOURNAL OF Evolutionary Biology eseb

Hybridization and transgressive exploration of wing morphology in Heliconius butterflies

Journal:	*Journal of Evolutionary Biology*
Manuscript ID	JEB-2019-00029
Manuscript Type:	Research Papers
Keywords:	diversification, mimicry, wing shape, colour pattern, Lepidoptera, Transgression, geometric morphometrics

Now published in Journal of Evolutionary Biology
Mérot C, Debat V, Le Poul Y, Merrill R, Naisbit R, Tholance A, Jiggins C, Joron M (2020) Hybridization and transgressive exploration of colour pattern and wing morphology in Heliconius butterflies. Journal of Evolutionary Biology. 13626 (6): 942-956
https://www.doi.org/10.1111/jeb.13626

Hybridization and transgressive exploration of wing morphology in *Heliconius* butterflies

Running title: Hybrid transgression of wing morphology

Key words: Wing shape – Colour pattern - Transgression – Geometric morphometry – Lepidoptera –Mimicry – Diversification

Abstract

Hybridization can generate novel phenotypes distinct from those of the parental lineages, a phenomenon known as transgression. Transgressive phenotypes might negatively or positively affect hybrid fitness, and increase genetic variation. Closely-related species of *Heliconius* butterflies produce 0.5–3% of natural hybrids and share genomic portions through gene flow. Introgression and the subsequent shuffling of major-effect loci may be involved in the evolution of new *Heliconius* wing colour patterns. However, the *Heliconius* wings are under strong stabilizing selection for mimicry, which limits within-species variance. Hybrid transgression may therefore play a role in exploring novel wing morphologies, not only regarding colour pattern but also shape or size. Here, by quantifying wing size, shape and colour pattern variation in hybrids from controlled crosses, we asked whether hybrids displayed transgressive wing morphologies. To investigate the effect of phenotypic proximity between parental lineages on transgression, we compared crosses between co-mimetic species to crosses between non-mimetic species. Analyses showed contrasted results depending on the underlying genetic architecture of traits and on the definition of transgression. Discrete traits underlain by major-effect loci, such as presence/absence of colour patches, generate novel phenotypes and high levels of transgression. For quantitative traits, such as wing shape or minute colour pattern details, hybrids rarely exceed the parental range, yet preferentially explore specific dimensions of the morphological space. Overall, our data suggests that the extent to which hybrid transgression contribute to phenotypic diversity is linked to the genetic architecture of the traits.

Introduction

Recent studies on phenotypic diversification reveal a more ambivalent role for hybridization than was previously recognised (Mallet, 2008; Hegarty, 2012; Abbott *et al.*, 2013; Yakimowski & Rieseberg, 2014; Meier *et al.*, 2017). Hybridization has classically been viewed as a force that homogenizes populations, acting against genetic differentiation, and preventing speciation (Mayr, 1963; Felsenstein, 1981). However, many species continue to hybridize throughout the process of speciation (Kronforst *et al.*, 2006b; Wiens *et al.*, 2006; Mallet *et al.*, 2007; Kulathinal *et al.*, 2009; Martin *et al.*, 2013), and increasing evidence suggests that a limited level of hybridization can instead represent a source of novel genetic variation, with possibly greater effects than mutation (Grant & Grant, 1994; Abbott *et al.*, 2013; Dittrich-Reed & Fitzpatrick, 2013).

Hybridization produces novel allelic combinations in hybrids, which may result in transgressive phenotypes that lie beyond natural variation expressed in parental populations (Rieseberg *et al.*, 1999; Stelkens *et al.*, 2009). Transgression has been reported for traits as diverse as mandible shape in mice (Renaud *et al.*, 2009; 2012), tolerance to temperature in copepods (Pereira *et al.*, 2014), and transcription level in fish (Czypionka *et al.*, 2012). When novel phenotypes are deleterious, reduced hybrid fitness forms a post-zygotic barrier, which can enhance pre-mating isolation through reinforcement, leading to species differentiation and ultimately diversification (Butlin, 1987a; Butlin, 1987b; Servedio & Noor, 2003; Smadja & Butlin, 2006). When novel phenotypes bear an adaptive value, in contrast, hybrids may backcross to parents and thus contribute to increasing the available genetic and phenotypic variation. This may influence the evolutionary trajectories of phenotypes in parental species (Selz *et al,* 2014), allowing, for instance, the colonization of new ecological niches (Nolte *et al.*, 2005; Hermansen *et al.*, 2011; Stemshorn *et al.*, 2011; Stelkens *et al.*, 2014; Meier *et al.*,

2017) or increasing within- and between-species phenotypic diversity (Gilbert, 2003; Mallet, 2009).

Hybrid transgression can have diverse genetic origins, including epistasis (Eshed & Zamir, 1996), overdominance (Rieseberg *et al.*, 1999), complementary action of additive alleles between multiple quantitative trait loci (Devicente & Tanksley, 1993; Rieseberg *et al.*, 1999; Rieseberg *et al.*, 2003; Albertson & Kocher, 2005; Stelkens & Seehausen, 2009; Stelkens *et al.*, 2009) or even epigenetics (Shivaprasad *et al.*, 2012). Theoretical predictions and empirical observations suggest that the degree of transgression depends on the phenotypic divergence between parental species. In particular, species that are phenotypically similar may be more likely than phenotypically more distinct species to accumulate complementary additive alleles which, summing up in hybrids, lead to transgression (Rieseberg *et al.*, 1999).

We here investigate the relationship between hybridization, adaptation and diversification in *Heliconius* butterflies. Hybridization is frequent between recently diverged species within the genus and results in a large fraction of the genome being shared between closely-related species (Mallet *et al.*, 2007; Martin *et al.*, 2013). Hybridization has been suggested as a critical factor in the evolution of *Heliconius* phenotypic diversity because inter-specific laboratory crosses generate a wide variety of wing patterns, a subset of which match natural patterns from other geographic areas (Gilbert, 2003). The importance of gene flow in the evolution of *Heliconius* is supported in nature by molecular evidence showing adaptive introgression of mimicry loci (Heliconius Genome Consortium, 2012; Pardo-Diaz *et al.*, 2012), sometimes followed by a shuffling between major-effect loci enhancing overall pattern diversity (Wallbank *et al.*, 2016; Enciso-Romero *et al.*, 2017). Here we use hybrids from laboratory crosses in *Heliconius* to investigate the effect of hybridization on wing shape and

colour pattern, two traits involved in Müllerian mimicry but displaying a different range of natural variation and likely based on different genetic architecture.

Wing colour pattern is a strikingly diversified trait in *Heliconius*. Wing pattern is under strong natural selection through its role as a warning signal involved in Müllerian mimicry (Mallet, 1989; Merrill *et al.*, 2012). The genetic architecture of wing pattern is shared across species and typically involves a limited number of large-effect loci switching on or off the presence of black shutters or colour patches in different compartments of the wing (Gilbert, 2003; Joron *et al.*, 2006; Kronforst *et al.*, 2006a; Baxter *et al.*, 2008; Ferguson *et al.*, 2010; Huber *et al.*, 2014; Wallbank *et al.*, 2016; Enciso-Romero *et al.*, 2017). Between species differing in colour pattern, hybridization usually reshuffles parental alleles, forming hybrids with a novel colour pattern that consists of a combination of elements of the parental patterns (Gilbert, 2003; Naisbit *et al.*, 2003). Such phenotypes generally do not sufficiently match either of the parental patterns that are recognised and avoided by predators, and so hybrids suffer from higher predation (Merrill *et al.*, 2012). This process strongly contributes to isolation between closely-related species (Jiggins *et al.*, 2001; Jiggins, 2008; Mallet, 2010). Yet, if the novel recombined pattern resembles other local patterns, or if hybrids are produced at a non-negligible frequency, hybridization may be a way to cross the fitness valley between adaptive peaks of mimicry, and by this process, hybridization may contribute to phenotypic diversification (Gilbert, 2003; Mavarez & Linares, 2008; Mallet, 2009; Merrill *et al.*, 2015).

Wing shape and size have received less attention than colour pattern because they appear more homogenous throughout the clade. However, experiments on flight and quantification of wing shape suggest that shape similarity between co-mimics is also favoured by selection (Srygley, 1999; Jones *et al.*, 2013; Mérot *et al.*, 2016). Contrary to colour pattern, for which

104 the genetic architecture is rather simple, shape is generally polygenic, involving interactions
105 between several loci (Zimmerman *et al.*, 2000; Navarro & Klingenberg, 2007; Klingenberg,
106 2010; Pitchers *et al.*, 2017). This makes it difficult to predict the effects of hybridization.
107
108 Geographical races of *Heliconius* allow us to contrast cases differing in the nature and degree
109 of divergence in parental morphology. Here we consider two pairs of species belonging to
110 sister clades: in Panama, *H. cydno chioneus* and *H. melpomene rosina* and in Peru, *H.*
111 *timareta thelxinoe* and *H. melpomene amaryllis* (Fig. 1A). *H. timareta* and *H. cydno* belong to
112 the same phylogenetic lineage, which diverged from *H. melpomene* about 2 million years ago
113 (Kozak *et al.*, 2014). Therefore, the two pairs involve similar duration of phylogenetic
114 divergence. However, phenotypic distances differ: the Peruvian *H. t. thelxinoe* and *H. m.*
115 *amaryllis* are co-mimics and exhibit a very similar colour pattern with a red forewing patch
116 and a yellow hindwing bar. In contrast, the Panamanian *H. c. chioneus* and *H. m. rosina* differ
117 in colour and pattern, mimicking two very distinct distantly-related *Heliconius* species (Fig.
118 1A). As a result, wing colour pattern, and likely wing shape, are under convergent selection in
119 the Peruvian co-mimetic pair (*H. m. amaryllis/H. t. thelxinoe*) and under divergent selection in
120 the Panamanian non-mimetic pair (*H. m. rosina/H. c. chioneus*). We can therefore investigate
121 the effect of parental phenotypic divergence upon the extent of hybrid transgression.
122
123 Transgression is the occurrence of extreme or novel phenotypes relative to the parental
124 phenotypes but, in the literature, it has been quantified in different ways, corresponding to
125 subtly different definitions. Transgression has been considered (1) as a deviation from a
126 linear intermediate between parental phenotypes, *i.e.* the mean hybrid value is not included in
127 the interval between the two parental means (Rieseberg *et al.*, 1999; Renaud *et al.*, 2012;
128 Renaud *et al.*, 2017), (2) or as the proportion of hybrids falling outside of the range of the

parental phenotypes (Rieseberg *et al.*, 1999; Parsons *et al.*, 2011; Holzman & Hulsey, 2017), (3) or as the expansion of the hybrid range beyond the range of the parental phenotypes (Stelkens *et al.*, 2009; Holzman & Hulsey, 2017; Husemann *et al.*, 2017).

We explore variation in wing size, shape and pattern, across parents, F1 and backcrosses in the two species pairs, to address the following questions: (1) What are the hybrid phenotypes and do they differ from parental morphologies? (2) To what extent do hybrids exhibit transgressive phenotypes and thereby explore novel wing morphologies? (3) Is the level of transgression dependent upon the phenotypic distance between parental species? In doing so, we explored three ways of measuring transgression and discuss the implications of choosing a given method (Fig. 1BCD).

Methods

Butterfly collection and crosses

Heliconius cydno chioneus (C) and *Heliconius melpomene rosina* (Mr) were collected from Gamboa, Republica de Panama. *Heliconius timareta thelxinoe* (T) and *Heliconius melpomene amaryllis* (Ma) were collected around Tarapoto, Peru (Fig. 1A). Field-caught mated females were used to establish stock populations of each taxon. For each sympatric pair, controlled crosses were performed to generate families of F1 hybrids ($F1_{C/Mr}$ in Panama, $F1_{T/Ma}$ in Peru) and backcross hybrids from crosses to both parental species (BC, backcross towards *H. c. chioneus,* BMr, backcross towards *H. m. rosina;* BT: backcross towards *H. t. thelxinoe*, BMa backcross towards *H. m. amaryllis,* Fig. 1A). Full details of the controlled crosses used here can be found elsewhere (Naisbit *et al.*, 2003; Merrill *et al.*, 2010; Mérot *et al.*, 2015; Merrill *et al.*, 2018).

Measurement of wing size, shape and pattern

Images of ventral (v) and dorsal (d) forewings (FW) and hindwings (HW) were captured using a Nikon D90 digital camera with a Nikon micro 105/2.8G ED VR lens. We retained only specimens with undamaged wings, resulting in the collection of data, for shape and pattern respectively, from 67 and 54 *H. c. chioneus* (C), 64 and 56 *H. m.rosina* (Mr), 33 and 31 $F1_{C/Mr}$, 169 and 144 BC, 101 and 88 BMr, 88 and 84 *H. m. amaryllis* (Ma), 70 and 66 *H. t. thelxinoe* (T), 42 and 42 $F1_{T/Ma}$, 50 and 51 BT, 175 and 169 BMa.

In total, 20 FW landmarks and 18 HW landmarks were used to quantify wing shape. Landmarks were placed at vein intersections and vein termini on the ventral side (Fig. S1) using TpsDig2 (Rohlf, 2010). Landmark coordinates were superimposed using a general Procrustes analysis (Bookstein, 1991; Zelditch *et al.*, 2004). A principal component analysis was applied to superimposed coordinates and the non-null PCs were used as shape descriptors in further analyses. Wing size was measured using centroid size [CS; see (Bookstein, 1991)].

Dorsal wing colour pattern was analysed using Colour Pattern Modelling (CPM) (Le Poul *et al.*, 2014). Briefly, wing outline was extracted individually from the background and, within this area, RGB colours were categorized into four colour classes (black, red, white or yellow) for each pixel. All individual wings were aligned by rotation, translation and scaling based on an iterative process maximizing overlap between pattern elements. This yields to wing surfaces characterized by a set of pixels with homologous position across specimens. Principal component analysis was applied to the set of pixels and the PCs were used as colour pattern descriptors in further analyses.

Following Husemann *et al.* (2017) and Stelkens *et al.* (2009), to remove sex-related effect, we performed a preparatory ANCOVA or MANCOVA with sex as factor and retained the residuals as variables for each of the six traits quantified (size, shape and colour pattern for the FW and HW). Because forewing and hindwing showed similar results, they were considered together, by summing the residuals for size, and by grouping all forewing and hindwing axes for either shape or pattern into two multivariate morphological matrixes (one for shape, one for pattern).

Differences in size between groups were investigated with a one-way analysis of variance (ANOVA), with *p*-values corrected for multi-test comparison following Benjamini and Hochberg (1995). Differences in shape and in pattern between groups were investigated with a one-way MANOVA with genotype as factor and respective PCs (shape or pattern) as dependent variables. PCA dimensionality was reduced following the Kaiser-Guttman criteria, *i.e.,* by keeping all PCs whose eigenvalues were above the average eigenvalue (Jackson, 2005).

Phenotypic distances between parental species

To quantify phenotypic distances between parental species (T *vs.* Ma, C *vs.* Mr*),* we worked on a subset including only individuals from parental species. Between all possible pairs of parental specimens, for size, we computed absolute differences in wing size, and, for shape or colour pattern, we measured Euclidian distances in PCAs applied on the parental subsets, truncated following the Kaiser-Guttman criteria (Jackson, 2005). To test whether parental distances differed between the mimetic and the non-mimetic pair, we applied a linear mixed model with individual distances as a variable, species pair (co-mimics/non-mimics) as a factor and identity of each sample as a random factor. Results were congruent when evaluated with Malahanobis distances between the four species (Table S1).

Analysis of hybrid phenotypic transgression

To quantify transgression in a meaningful morphospace, we translated the two morphological matrices (pattern and shape) into 12 subset morphospaces by applying a PCA on a subset with 3 genotypes, *i.e.,* the target hybrid population H (F1 hybrids or either backcross hybrids) and its parental species (for instance the target hybrid population is BC and the parental populations are C and Mr), further truncated following the Kaiser-Guttman criteria (Jackson, 2005). Transgression was then quantified with three indices corresponding to different definitions of transgressive segregation used in the recent literature for multivariate data.

- Transgression of the mean (Fig. 2B)

Renaud *et al.* (2012); Renaud *et al.* (2017) proposed that in the absence of transgression, the average hybrid phenotype should be strictly intermediate between parental groups. In that case the sum of the distances between the mean hybrid and the two parents ($d(H,P_1) + d(H,P_2)$) should be equal to the distance between the parents $d(P_1,P_2)$.

Transgression of the mean could thus be assessed as the departure of the mean hybrid phenotype from this expectation:

$$T_m = \frac{d(H,P_1) + d(H,P_2) - d(P_1,P_2)}{d(P_1,P_2)}$$

Where $d(H,P_1)$ and $d(H,P_2)$ are the Euclidian distances between the mean hybrid phenotype and the mean phenotype of the first and second parent, respectively, and $d(P_1,P_2)$ is the Euclidian distance between the mean parental phenotypes.

- Range transgression (Fig. 2C)

Parsons *et al.* (2011) considered transgression in relation to the frequency of transgressive hybrids, *i.e.,* hybrids whose trait value exceeded a certain distance from the parental mean trait. Here, following traditional definition of transgression (Rieseberg *et al.*, 1999), and the "proportional expansion index" defined in Holzman (2017), we chose that distance to be the parental range. In the multivariate data, the range was defined as the maximal Euclidian distance in the morphospace between a parental phenotype (P_i) and its consensus (P_1 for parent 1 or P_2 for parent 2).

A hybrid was thus be considered transgressive when its Euclidian distance in the morphospace to both parental means was greater than the given parental range, *i.e.,* if the distance between the hybrid H_i and each of the parents (P_1 and P_2) meets the following two conditions:

$$d(H_i,P_1) > Max\,(d(P_i,P_1))$$

&

$$d(H_i,P_2) > Max\,(d(P_i,P_2))$$

The index of range transgression (*Tr*) was calculated as the frequency of transgressive hybrids.

- Transgression strength (Fig. 2D)

Stelkens *et al.* (2009), followed by Husemann *et al.* (2017) and Holzman and Hulsey (2017) which call this measure "distance expansion", proposed to evaluate the degree of transgression by evaluating to what extent hybrid range exceeds the parental range. In multivariate data, range was calculated as the difference between the minimal and the

maximal value along each PC, and transgression strength was first evaluated on each PC separately following Stelkens *et al.* (2009):

$$Ts\ (PC_i) = \frac{(total\ range\ along\ PC_i - parental\ range\ along\ \ PC_i\ )}{parental\ range\ along\ PC_i}$$

A global index of the strength of multidimensional transgression (*Ts*) was then estimated as the sum of these values, weighted by the variance explained by each PC:

$$Ts = \sum_i \frac{(total\ range\ along\ PC_i - parental\ range\ along\ \ PC_i\ )}{parental\ range\ along\ \ PC_i} * Var\ (PC_i)$$

To compare the transgression index against a null model, each index was compared to a distribution of the transgression index built by simulating 1000 populations of hybrids built as a linear combination of the parental phenotype. More specifically, the trait of each simulated hybrid was calculated as the weighted mean trait of two randomly chosen parents: $F_1 = \frac{P_1 + P_2}{2}$; $BP_1 = \frac{3P_1 + P_2}{4}$; $BP_2 = \frac{P_1 + 3P_2}{4}$. The simulated hybrid population was of the same sample size as the corresponding experimental population. Then, to evaluate the effect of unbalanced sample size, we also re-calculated each index 1000 times by drawing randomly 30 individuals in each experimental group (P1, P2, H) and reported the mean and standard deviation of this distribution. This was compared to the null distribution of the transgression index calculated again on 1000 populations of theoretically non-transgressive hybrids but with sample size fixed to 30.

271 To visualise the directions of maximal variation between parents and hybrids, as well as the
272 direction of transgression, we used a between-group PCA (bg-PCA) (Boulesteix, 2005;
273 Mitteroecker & Bookstein, 2011).
274
275 All analyses were performed in R 3.1 (R Core Team, 2014), using the libraries *lme4* (Bates *et*
276 *al.*, 2013), *ade4* (Dray & Dufour, 2007) and *Rmorph* (Baylac, 2012).

Results

Phenotypic distances in parental species

The parental species in both pairs differed significantly in size, shape and pattern (Table S1). *H. timareta thelxinoe* and *H. cydno* were larger than *H. melpomene* (Fig. 2). They had a more elongated forewing with a shorter discal cell and a wider hindwing compared to *H. melpomene* (Fig. 3A-B, Fig. S3). Despite being co-mimetic, *H. melpomene amaryllis* and *H. timareta thelxinoe* differed in pattern, with subtle variation in the position and morphology of the colour patches (Fig. 3C, Fig. S4). Overall phenotypic distances were significantly smaller between mimetic *H. m. amaryllis/H. t. thelxinoe* than between non-mimetic *H. m. rosina/H. cydno,* by a factor of 1.3 for wing size ($F_{1,135} = 16$, $p < 0.001$), 1.2 for wing shape ($F_{1,135} = 60$, $p < 0.001$) and 3.1 for pattern ($F_{1,118} = 3896$, $p < 0.001$), indicating not only similarity of pattern between co-mimics but also increased similarity of wing shape and size (Fig. S2, Table S1).

Hybrid phenotype and transgression

Wing size

For both the Peruvian and the Panamanian sets, forewing and hindwing centroid size of hybrids were intermediate between the smaller *H. melpomene* and the larger *H. cydno/H. timareta* (Fig. 2). Hybrid sizes were generally ordered according to the genetic contribution of parental species.

Transgression of the mean was null for all hybrid groups, except for BT, which exhibited a positive transgression of the mean (0.12). Few hybrids fell outside of parental wing size ranges. Range transgression and transgression strength were null, except for some very weak values in BMr ($Tr = 0.01$, $Ts = 0.1$) and BMa ($Tr = 0.01$, $Ts = 0.01$).

Wing shape

Hybrid wing shapes were significantly different from parental shapes, both for the mimetic and the non-mimetic crosses (Table S2). In both crosses, shape variation in forewing and hindwing was dominated by the differentiation of the parental species (bgPC1, 73–76% of shape variance; Fig. 3A,B). *H. melpomene* forewing and hindwing had a longer discal cell and a shorter, rounded distal region of the wing compared to *H. cydno* or to *H. timareta*. Along this axis of variation, driven by inter-specific parental divergence, wing shapes of hybrids were intermediate, staying within the overlapping parental ranges, with backcrosses closer to their majority parent. Along the second and third axes of the bgPCA describing 20–25% of variance, a slight transgressive effect was observed, with the group of hybrids deviating from the expected inter-parental position.

This shifted position is associated with positive transgression of the mean wing shape, significantly higher than expected in simulated non-transgressive hybrids (Table 1). Transgression of the mean was higher in backcrosses between the co-mimics (BMa*:* $Tm = 0.27$, BT: $Tm = 0.44$) than in backcrosses between non-mimics (BMr: $Tm = 0.16$, BC: $Tm = 0.16$), and this difference held true when controlling for parental distance ratio (Table S4). In contrast, the range transgression index was very low and similar between all groups, with less than 1% of hybrids outside the parental ranges (except $F1_{C/Mr}$: $Tr = 0.03$). Transgression strength was also low and comparable between all groups when summing all dimensions (*Ts* ranges between 0.02 and 0.06), but significantly higher than in the simulated hybrids. The strength of transgression varied widely depending on the PC considered (Table S3), from 0, when hybrids did not exceed parental ranges, to 0.08–0.38, indicating that

hybrids exceeded parental range by 8–38% in some directions of the shape space, for instance on the second or third PCs (representing about 10-15% of variance).

Wing colour pattern

For the mimetic Peruvian pair, parents and hybrids present the same general features, a black background with a red forewing patch and a yellow hindwing band. Despite this, there is significant variation in the morphology and the position of colour patches between parents and hybrids (Table S2, Fig. 3C, Fig. S4). Most of the between-group variation, represented by bg-PC1 (65% of variance), corresponds to differences between parents. The *H. timareta thelxinoe* forewing red patch is narrower, with a somehow zigzagging shape, and its yellow hindwing bar is narrower than that of *H. melpomene amaryllis* (Mérot *et al.*, 2013). Along this axis of variation, hybrids are mostly intermediate and within the partially-overlapping parental range. Along the second and third bg-PC, hybrids displayed a transgressive pattern that is not observed in parents.

For the non-mimetic Panamanian pair, as previously described (Naisbit *et al.*, 2003), F1 hybrids and some of the backcross individuals displayed a pattern that was never found in parents, recombining white and red in the forewing bar and showing a completely black hindwing (Fig. 3D, Fig. S4). This transgressive pattern falls between the two non-overlapping parental ranges on bg-PC1 and dominates the second bg-PC. Beyond the presence/absence of colour patches, there was also large variability within backcross groups in the position and size of colour patches (Fig. 3D, Fig. S4).

For hybrids from both sets of crosses, transgression of the mean colour pattern was significantly higher than expected in the simulated non-transgressive hybrids (Table 1).

Transgression of the mean was higher in backcrosses between co-mimics (BMa: *Tm* = 0.41; BT: *Tm* = 0.42) than in backcrosses between non-mimics (BMr: *Tm* = 0.22; BC: *Tm* = 0.21), but this difference was not observed when controlling for the ratio of parental distances (Table S4). Range transgression is higher for wing pattern than for shape in both pairs and much higher for the non-mimetic pair than for the mimetic pair (Table 1). Only 5–10% of hybrids between the mimetic pair T/Ma fall outside of the parental ranges, while for the non-mimetic C/Mr pair, 71% to 83% of the backcrosses and 100% of F1 lie outside of the parental ranges. Transgression strength is also much higher in the non-mimetic pair than in the mimetic pair. Again, within the overall index, it is worth noting that, along certain directions of variation (several PCs explaining 2-10% of variance), mimetic hybrids exceed the parental range by up to 44% and non-mimetic hybrids by up to 330% (Table S3).

Discussion

Overall, the precise quantification of morphology in hybrids demonstrates the variable consequences of hybridization. Wing size is largely intermediate between parental phenotypes; hybrid wing shape deviates from the expected intermediate position between the parental shapes; colour pattern also deviates from an intermediate position and sometimes displays complete novelty compared to parents, particularly in the cross between non-mimetic species. The level of transgression therefore clearly varies among traits. This variation may reflect trait complexity, genetic architecture, and the phenotypic distances between parents. Furthermore, different methods of defining and quantifying transgression show different patterns and influence our conclusions with regard to the degree to which hybridization generates transgression and the influence of parental phenotypic similarity.

Transgression and novelty in hybrid phenotypes

In complex traits such as many morphological traits, transgression is expected and frequently observed in hybrids (Rieseberg *et al.*, 1999; Rieseberg *et al.*, 2003; Stelkens & Seehausen, 2009; Stelkens *et al.*, 2009; Parsons *et al.*, 2011; Renaud *et al.*, 2012; Selz *et al.*, 2014; Holzman & Hulsey, 2017; Husemann *et al.*, 2017; Renaud *et al.*, 2017). Here, we have shown that size, a univariate trait, shows nearly no transgressive effect, whereas multivariate traits such as shape and pattern show much more marked transgression. This may perhaps be due to an increasing range of possibilities for transgression when a greater number of dimensions of variation contribute to the phenotype.

The extent of hybrid transgression also depends on which definition of transgression is used. Indeed, indices that consider the mean and the range actually address different hypotheses. Transgression of the mean evaluates the extent to which the mean phenotype of all hybrid offspring is different from an intermediate phenotype lying between the parental means. It actually tests a deviation from a genetic additive linear model, and whether a preferential direction of deviation is explored by the hybrids as a group but not individual novelty. In contrast, the range transgression, and transgression strength, test the extent to which the phenotypic range of hybrid exceeds parental ranges, in other words to what extent novel phenotypes are produced in hybrids.

The different indices provided congruent values of high transgression only for colour pattern of non-mimetic hybrids. In contrast, wing shape (both pairs) and colour pattern (co-mimetic pair), showed intermediate values of transgression of the mean but almost null range transgression. In the latter case, this means that few of the hybrids display phenotypes outside the parental ranges, yet the majority of the hybrids deviate from a pure intermediate. Such

deviation is missed by our range index, which supposes isotropy (equal variations in all directions), but it is captured by the second axis of the bg-PCA and by observing, in the index of transgression strength, a transgressive effect associated with some morphological directions. The fact that some directions of morphological transgression are occupied by a group of hybrids means that, although, individually, few hybrids represent new phenotypes, some hybrid morphologies are produced at a higher probability. This possibly reveals genetic interactions due to hybridization and a non additive/non-linear underlying genetic architecture and may also represent the most available and heritable directions of morphological variation.

Hybrid novelty and genetic architecture of wing morphology

The traits considered in this study rely on different genetic mechanisms, which likely explain the differences in transgressive effect. Patterns in hybrids between the non-mimetic Panamanian species, *H. melpomene rosina* and *H. cydno chioneus,* are totally new because they recombine discrete elements of parental colour pattern (such as black "shutters" or large colour patches) whose presence is controlled by unlinked loci of major effect in parental species (Martin *et al.*; Mallet, 1989; Gilbert, 2003; Naisbit *et al.*, 2003; Jiggins *et al.*, 2005; Joron *et al.*, 2006; Martin *et al.*, 2012; Huber *et al.*, 2014). Dominance at those loci is strong and several loci are found in linkage, leading to the segregation within the back-crosses of phenotypes that are either F1-like or similar to one of the parental phenotypes (Naisbit *et al.*, 2003). For example, the presence of a red forewing patch is associated with the *B* locus that is expressed in *H. melpomene* and hybrids carrying the dominant *B* allele, while no red patch is observed in *H. cydno* and backcrosses with *bb* genotype.

In contrast, the red patch of *H. melpomene amaryllis, H. timareta thelxinoe* and their hybrids are controlled by the same *B* locus, introgressed between the species (Heliconius Genome Consortium, 2012; Pardo-Diaz C. *et al.*, 2012), and no effects of dominance on hybrid

variation is expected. Yet, our projection of hybrid phenotype in the morphospace shows that the position and the morphology of colour patches vary between species and in hybrids. This suggests that subtle variations in colour pattern involve additional small-effect quantitative loci, which may affect the accuracy of mimicry, and are expected to produce transgressive phenotypes in hybrids. Such subtle variation in the position and morphology of the colour patch is also observed in the non-mimetic pair in addition to the presence/absence of colour patches. This subtle variation has been partly attributed to epistatic interactions between heterospecific colour pattern major-effect genes (Naisbit *et al.*, 2003) and may also involve small-effect loci. For instance, in *H. melpomene,* the morphology of the red forewing patch has been associated with several QTLs on different chromosomes and distinct from the major switch genes (Baxter *et al.*, 2008).

The genetic basis of wing shape is completely unknown in *Heliconius*. Generally, shape is a complex trait involving multiple small-effect loci, e.g., in *Drosophila* (Pitchers *et al.*, 2017). Here, in both sets of crosses, between co-mimics or non-mimics, hybrid wing size and shape are largely intermediate between parental phenotypes. Backcross individuals are generally closer to the phenotype of the parental species representing the majority of the ancestors (BT is closer to *H. t. thelxinoe* than to *H. melpomene amaryllis,* for instance). This suggests an additive genetic basis for wing shape, possibly with complementary additive alleles underlying transgression and stronger effects of certain alleles determining the preferential directions explored in hybrids.

Transgressive effect and parental similarity

When transgression is due to the complementary action of multiple additive alleles that are present in parental lines, it is predicted that transgression is higher in phenotypically similar

taxa (Rieseberg, 1999). This is because a polygenic trait under stabilizing selection involves multiple loci with opposing effects (within species), but not necessarily the same alleles and the same directional effect in two phenotypically similar species. In hybrids between phenotypically similar parents, the different effects can thus sum for several genes, resulting in high transgression. In contrast, dissimilar parental phenotypes, evolving under directional or divergent selection, are expected to accumulate alleles driving phenotypic variation consistently in opposing directions, which then cancel each other in hybrids (Rieseberg *et al.*, 1999; Rieseberg *et al.*, 2003; Albertson & Kocher, 2005; Stelkens & Seehausen, 2009).

This prediction is rather appropriate to highly-polygenic traits involving multiple small-effect loci (Rieseberg *et al.*, 1999; Stelkens *et al.*, 2014), such as wing shape or size. Our results confirm that the mimetic parents are more similar in shape and size than non-mimetic species, suggesting that mimicry goes beyond colour pattern and might include shape and size, and perhaps therefore flight behaviour. Our prediction was that transgression for size and shape should be higher in crosses between co-mimics than between non-mimics. Results provided mixed support for this. On the one hand, in both pairs of species, size was generally not transgressive, and shape displayed low or null transgression when considering indexes based on the range. On the other hand, wing shape does display a higher transgression of the mean in the co-mimetic pair than in the non-mimetic pair. This could confirm the polygenic nature of wing shape and would deserve further investigation.

In contrast, for wing pattern, transgression was higher in hybrids between non-mimics than between co-mimics. This is probably not surprising given that pattern involves few large-effect loci operating in different compartments and with dominance relationships, and hybrids between non-mimetic parents were expected generally to be very different from the parents.

Altogether, comparing the species pairs and separating the different morphological components of the visual wing phenotype, our results confirms that hybrid transgression is a complex phenomenon which is difficult to predict due to the variation in genetic architectures underlying those different traits.

Hybrid wing morphology and fitness

Wing morphology is a key component of adaptation in *Heliconius* butterflies because of Müllerian mimicry (Mallet & Gilbert, 1995). Mimicry relies on the fact that predators learn to associate unpalatability with a previously encountered warning signal. Thus, resemblance between chemically-defended species coexisting in the same habitat contributes to enhancing the protection conferred by the local warning signal (Müller, 1879; Turner, 1977). Exotic or novel patterns generally suffer from higher attack rates (Langham, 2004; Arias *et al.*, 2016). For instance, F1 hybrids between *H. melpomene rosina* and *H. cydno chioneus,* which combine red and white on the forewing and form a novel pattern*,* suffer from higher predation than parental patterns, and this contributes to reproductive isolation (Merrill *et al.*, 2012). However, we note that in certain cases, patterns not mimicking any known species in their local community may persist in the wild. This is the case, for instance, for the Colombian species, *Heliconius heurippa,* whose very prominent red and yellow forewing patch is not found in any coexisting species. This pattern is very similar to the one observed here in hybrids between *H. cydno* and *H. melpomene*, and is an example of pattern novelty produced via hybridization and introgression (Mavarez *et al.*, 2006; Pardo-Diaz C. *et al.*, 2012).

Because the same "toolbox" of major-effect colour pattern loci is re-used in the different *Heliconius* species, hybrid phenotypes may in fact match co-existing warning patterns and benefit from their protection (Gilbert, 2003; Enciso-Romero *et al.*, 2017). A fraction of the

back-crosses between the non-mimetic Panamanian species present an overall pattern that roughly mimics one of the parents (Naisbit *et al.*, 2003). Yet, subtle variation in the morphology or position of the colour patches makes them imperfect mimics. Similarly, hybrids between the Peruvian co-mimics are very similar at first sight with both of the parents and within the overall parental range, but they slightly deviate from the parental patterns. As for wing shape and size, subtle phenotypic differences possibly translate into differences in fitness. In *H. timareta thelxinoe,* within-species geographic variation tend to follow the most abundant warning pattern in the local community, mimicking the abundant *H. erato favorinus/H. melpomene amaryllis* at mid-altitude and another species, *H. telesiphe,* at high altitude (Mérot *et al.*, 2016). *H. telesiphe* has narrower colour bands and a Z-shaped FW pattern which are not readily mimicked by the hybrids between *H. t. thelxinoe* and *H. m. amaryllis,* but the hybrids are more similar to *H. m. amaryllis* Therefore, depending on the surrounding community, hybrids are either better or worse mimics than their parents.

Depending on the extent of selection on wing morphology, possibly linked to the degree of generalization by bird predators or the local community of mimics, hybrid phenotypes may thus be disadvantageous or advantageous. If disadvantageous, it may reinforce species isolation. If neutral or advantageous, for instance if the hybrid phenotype includes discrete elements of co-occurring warning pattern or subtle improvements of mimicry accuracy, variations displayed in hybrids can spread morphological possibilities in parental species and contribute to phenotypic evolution. In *Heliconius,* this mechanism of novelty by hybridization is thought to be more important than novelty by mutation, since a large portion of pattern diversity observed in *Heliconius* (at least in the *cydno-melpomene* subclade) can be explained by interspecific introgression and a re-shuffling of the different loci regulating each sub-elements of the pattern (Gilbert, 2003; Wallbank *et al.*, 2016; Enciso-Romero *et al.*, 2017).

Nothing is known, however, about other components of wing morphology involved in mimetic accuracy, such as subtle variations of the pattern or wing shape and size, which, given the extent of interspecific genome sharing, may also have partly evolved with input from hybridization.

Conclusion

Overall, our study reveals that the occurrence and the extent of transgression depend on the genetic architecture of the trait. Completely novel phenotypes were only found for the wing colour pattern of non-mimetic hybrids, due to the shuffling of alleles at unlinked large-effect genes, switching on and off the components of colour pattern. In contrast, for traits with more likely polygenic and quantitative variation, such as wing shape or wing colour pattern in the co-mimetic pair, hybrid phenotypes were generally within the range of parental phenotypes. However, in that case, the average hybrid morphology was distinct from a truly intermediate phenotype and transgressive along particular directions in the morphological space, perhaps revealing the underlying bias in the genetic architecture of the traits. In the mimetic species studied here, mimicry has been achieved by the introgression of at least a few large-effect loci controlling colour pattern loci. Whether more loci, affecting for instance the accuracy of mimicry, have also flowed among species and were positively selected is yet unknown. Here we focused on two pairs of butterfly species through the prism of mimicry, because selective factors associated with mimicry are well understood. Yet, any functional trait shared between species still exchanging gene flow also evolves in a multi-species context, with rare hybrids offering transgressive phenotypes and new combination of traits to selection. This raises the question to what extent occasional hybridization intervenes in evolution, by increasing standing variation, either with subtle changes or largely novel variation.

548 **Table 1. Transgression in hybrids.**

549 Each index (left column) is calculated for wing shape and wing pattern for the F1 and
550 backcrosses from the non-mimetic (*H. t. thelxinoe* [T] and *H. m. amaryllis* [Ma]) and mimetic
551 (*H. c. chioneus* [C] and *H. m. rosina* [Mr]) crosses. Indices based on 30 randomly-chosen or
552 simulated hybrids were based on 1000 bootstraps. Stars indicate the probability that the
553 observed values of the transgression indices were drawn from the simulated distribution of
554 theoretically non-transgressive hybrids; ** $p < 0.001$ and * $p < 0.01$.

555

			Index based on all samples	**Mean index (sd), 30 randomly-chosen samples**	**Mean index (sd), 30 simulated hybrids**		**Index based on all samples**	**Mean index (sd), 30 randomly-chosen samples**	**Mean index (sd), 30 simulated hybrids**
Transgression of the mean (*Tm*)	pattern	BMa	0.41**	0.45 (0.13)	0.08 (0.04)	BMr	0.22**	0.22 (0.03)	0.00 (0.00)
		$F1_{TMa}$	0.27**	0.30 (0.07)	0.05 (0.03)	$F1_{CMr}$	0.48**	0.48 (0.02)	0.00 (0.00)
		BT	0.42**	0.46 (0.11)	0.08 (0.05)	BC	0.21**	0.21 (0.04)	0.00 (0.00)
	shape	BMa	0.27**	0.38 (0.12)	0.14 (0.07)	BMr	0.16**	0.20 (0.05)	0.07 (0.04)
		$F1_{TMa}$	0.20**	0.27 (0.07)	0.09 (0.04)	$F1_{CMr}$	0.22**	0.25 (0.05)	0.04 (0.02)
		BT	0.44**	0.48 (0.11)	0.12 (0.06)	BC	0.16**	0.22 (0.06)	0.07 (0.03)
Range Transgression (*Tr*)	pattern	BMa	0.10**	0.12 (0.07)	0.00 (0.00)	BMr	0.83**	0.81 (0.06)	0.43 (0.10)
		$F1_{TMa}$	0.05**	0.15 (0.06)	0.00 (0.00)	$F1_{CMr}$	1.00	1.00 (0.00)	1.00 (0.01)
		BT	0.08**	0.12 (0.08)	0.00 (0.00)	BC	0.71**	0.73 (0.08)	0.15 (0.14)
	shape	BMa	0.01**	0.02 (0.02)	0.00 (0.00)	BMr	0.01**	0.01 (0.02)	0.00 (0.00)
		F1TMa	0.00	0.01 (0.02)	0.00 (0.00)	$F1_{CMr}$	0.03**	0.05 (0.03)	0.00 (0.00)
		BT	0.00	0.01 (0.03)	0.00 (0.00)	BC	0.02**	0.04 (0.04)	0.00 (0.00)
Transgression Strength (*Ts*)	pattern	BMa	0.09**	0.06 (0.03)	0.00 (0.00)	BMr	0.51**	0.34 (0.04)	0.00 (0.00)
		$F1_{TMa}$	0.02**	0.06 (0.02)	0.00 (0.00)	$F1_{CMr}$	0.40**	0.32 (0.03)	0.00 (0.00)
		BT	0.01*	0.03 (0.01)	0.00 (0.00)	BC	0.45**	0.36 (0.01)	0.00 (0.00)
	shape	BMa	0.06**	0.05 (0.03)	0.01 (0.01)	BMr	0.04**	0.03 (0.01)	0.00 (0.00)
		$F1_{TMa}$	0.01**	0.04 (0.02)	0.00 (0.00)	$F1_{CMr}$	0.02**	0.04 (0.02)	0.00 (0.00)
		BT	0.01**	0.03 (0.02)	0.01 (0.01)	BC	0.06**	0.04 (0.02)	0.00 (0.00)

556

Figure 1. Study species and methods.

(A) Phylogenetic relationship between the parental species, map of repartition, parental phenotypes and design of the crosses. Between Peruvian mimetic parents: $F1_{T/Ma}$, first generation hybrids between *H. t. thelxinoe* and *H. m. amaryllis;* BT, backcross with *H. t. thelxinoe;* BMa, backcross with *H. m. amaryllis.* Between Panamanian non-mimetic parents: $F1_{C/Mr}$, first generation hybrids between *H. c. chioneus* and *H. m. rosina;* BC, backcross with *H. c. chioneus;* BMr, backcross with *H. m. rosina*. (**B-D**) Illustrations of alternative measures of hybrid transgression. **(B)** Transgression of the mean, measured as the departure of the mean hybrid phenotype from that of the two parental phenotypes, relative to the distance between the parents (based on Renaud *et al.* (2012); Renaud *et al.* (2017)). **(C)** Range transgression, in which transgressive hybrids are those for which the distance from the parental phenotypes exceeds the parental range (based on Parsons *et al.* (2011)). **(D)** Transgression strength along principal component axes, measured as the extent to which hybrid range extends beyond the range of parental phenotypes (based on Stelkens *et al.* (2009) and Husemann *et al.* (2017)).

Figure 2. Wing size distribution of hybrids and parents.

Boxes indicate quartile, notches are 95% confidence intervals of the median, whiskers extend to maximal values. Shared letters indicate groups that do not differ significantly in wing size. All groups were tested together with a pairwise t-test corrected following Benjamini and Hochberg (1995).

Figure 3. Variation of hybrid wing shape and pattern.

Bg-PCA on forewing and hindwing shape for parental specimens, F1 and backcross hybrids between *H. timareta thelxinoe* and *H. melpomene* **(A)** and between *H. cydno chioneus* and *H. melpomene rosina* **(B)**. Shape variation is illustrated for each axis, where red broken lines represent minimum negative values of the axis, and full black lines represent maximum values.

Bg-PCA on forewing and hindwing pattern for hybrids between *H. timareta thelxinoe* and *H. melpomene* **(C)** and between *H. cydno chioneus* and *H. melpomene rosina* **(D).** Open circles represent males and filled dots represent females.

Abbott, R., Albach, D., Ansell, S., Arntzen, J.W., Baird, S.J.E., Bierne, N., et al. 2013. Hybridization and speciation. *J. Evol. Biol.* **26:** 229-246.

Albertson, R.C.Kocher, T.D. 2005. Genetic architecture sets limits on transgressive segregation in hybrid cichlid fishes. *Evolution* **59:** 686-690.

Arias, M., le Poul, Y., Chouteau, M., Boisseau, R., Rosser, N., Théry, M., et al. 2016. Crossing fitness valleys: empirical estimation of a fitness landscape associated with polymorphic mimicry. *Proc. R. Soc. B-Biol. Sci.* **283:** 20160391.

Bates, D., Maechler, M., Bolker, B.Walker, S. 2013. lme4: Linear mixed-effects models using Eigen and S4. R package version 1.0-4. *Accessed online*.

Baxter, S.W., Johnston, S.E.Jiggins, C.D. 2008. Butterfly speciation and the distribution of gene effect sizes fixed during adaptation. *Heredity***:** 1-9.

Baylac, M. 2012. Rmorph: a R geometric and multivariate morphometrics library. *Available from the author: baylac@mnhn.fr*.

Benjamini, Y.Hochberg, Y. 1995. Controlling the false discovery rate - A practical and powerful approach to multiple testing. *J. Roy. Stat. Soc. Ser. B. (Stat. Method.)* **57:** 289-300.

Bookstein, F., ed. 1991. *Morphometrics tools for landmark data: geometry and biology*. New York, NY: Cambridge University Press.

Boulesteix, A.-L. 2005. A note on between-group PCA. *International Journal of Pure and Applied Mathematics* **19:** 359–366.

Butlin, R. 1987a. Speciation by reinforcement. *Trends Ecol. Evol.* **2:** 8-13.

Butlin, R.K. 1987b. Species, speciation and reinforcement. *Am. Nat.* **130:** 461-464.

Czypionka, T., Cheng, J., Pozhitkov, A.Nolte, A.W. 2012. Transcriptome changes after genome-wide admixture in invasive sculpins (Cottus). *Mol. Ecol.* **21:** 4797-4810.

Devicente, M.C.Tanksley, S.D. 1993. QTL analysis of transgressive segregation in an interspecific tomato cross. *Genetics* **134:** 585-596.

Dittrich-Reed, D.R.Fitzpatrick, B.M. 2013. Transgressive hybrids as hopeful monsters. *Evol. Biol.* **40:** 310-315.

Dray, S.Dufour, A.-B. 2007. The ade4 package: implementing the duality diagram for ecologists. *Journal of statistical software* **22:** 1-20.

Enciso-Romero, J., Pardo-Díaz, C., Martin, S.H., Arias, C.F., Linares, M., McMillan, W.O., et al. 2017. Evolution of novel mimicry rings facilitated by adaptive introgression in tropical butterflies. *Mol. Ecol.* **26:** 5160-5172.

Eshed, Y.Zamir, D. 1996. Less-than-additive epistatic interactions of quantitative trait loci in tomato. *Genetics* **143:** 1807-1817.

Felsenstein, J. 1981. Skepticism towards Santa Rosalia, or why are there so few kinds of animals?. Evolution, 124-138. *Evolution* **35:** 124-138.

Ferguson, L., Lee, S.F., Chamberlain, N., Nadeau, N., Joron, M., Baxter, S., et al. 2010. Characterization of a hotspot for mimicry: assembly of a butterfly wing transcriptome to genomic sequence at the HmYb/Sb locus. *Mol. Ecol.* **19:** 240-254.

Gilbert, L. 2003. Adaptive novelty through introgression in Heliconius wing patterns: evidence for shared genetic "tool box" from synthetic hybrid zones and a theory of diversification. *Ecology and evolution taking flight: butterflies as model systems***:** 281-318.

Grant, P.R.Grant, B.R. 1994. Phenotypic and genetic effects of hybridization in Darwin's finches. *Evolution* **48:** 297-316.

Hegarty, M.J. 2012. Invasion of the hybrids. *Mol. Ecol.* **21:** 4669-4671.

Heliconius Genome Consortium 2012. Butterfly genome reveals promiscuous exchange of mimicry adaptations among species. *Nature* **487:** 94-98.

Hermansen, J.S., Saether, S.A., Elgvin, T.O., Borge, T., Hjelle, E.Saetre, G.P. 2011. Hybrid speciation in sparrows I: phenotypic intermediacy, genetic admixture and barriers to gene flow. *Mol. Ecol.* **20:** 3812-3822.

Holzman, R.Hulsey, C.D. 2017. Mechanical transgressive segregation and the rapid origin of trophic novelty. *Scientific reports* **7:** 40306.

Huber, B., Whibley, A., Poul, Y.L., Navarro, N., Martin, A., Baxter, S., et al. 2014. Conservatism and novelty in the genetic architecture of adaptation in Heliconius butterflies. *Heredity*.

Husemann, M., Tobler, M., McCauley, C., Ding, B.Danley, P.D. 2017. Body shape differences in a pair of closely related Malawi cichlids and their hybrids: Effects of genetic variation, phenotypic plasticity, and transgressive segregation. *Ecol. Evol.* **7:** 4336-4346.

Jackson, J.E. 2005. *A user's guide to principal components*. John Wiley & Sons, New York.

Jiggins, C.D., Naisbit, R.E., Coe, R.L.Mallet, J. 2001. Reproductive isolation caused by colour pattern mimicry. *Nature* **411:** 302-305.

Jiggins, C.D., Mavarez, J., Beltran, M., McMillan, W.O., Johnston, J.S.Bermingham, E. 2005. A genetic linkage map of the mimetic butterfly *Heliconius melpomene*. *Genetics* **171:** 557-570.

Jiggins, C.D. 2008. Ecological speciation in mimetic butterflies. *Bioscience* **58 No 6:** 541-548.

Jones, R., Poul, Y.L., Whibley, A., Mérot, C., FFrench-Constant, R.Joron, M. 2013. Wing shape variation associated with mimicry in butterflies. *Evolution* **67(8),:** 2323-2334.

Joron, M., Papa, R., Beltràn, M., Chamberlain, N., Malvarez, J., Baxter, S., et al. 2006. A conserved supergene locus controls colour pattern diversity in *Heliconius* Butterflies. *PLoS Biol.* **4**.

Klingenberg, C.P. 2010. Evolution and development of shape: integrating quantitative approaches. *Nat. Rev. Genet.* **11:** 623-635.

667 Kozak, K.M., Wahlberg, N., Neild, A., Dasmahapatra, K.K., Mallet, J.Jiggins, C.D. 2014.
668 Multilocus Species Trees Show the Recent Adaptive Radiation of the Mimetic
669 Heliconius Butterflies. *Systematic biology* **syv007**.
670 Kronforst, M.R., toung, L.G., Kapan, D.D., MCNeely, C., O'Neill, R.J.Gilbert, L.E. 2006a.
671 Linkage of butterfly mate preference and wing color preference cue at the genomic
672 location of wingless. *Proc. Natl. Acad. Sci. USA* **103:** 6575-6580.
673 Kronforst, M.R., Young, L.G., Blume, L.M.Gilbert, L.E. 2006b. Multilocus analyses of
674 admixture and introgression among hybridizing *Heliconius* butterflies. *Evolution* **60:**
675 1254-1268.
676 Kulathinal, R.J., Stevison, L.S.Noor, M.A.F. 2009. The genomics of speciation in drosophila:
677 diversity, divergence, and introgression estimated using low-coverage genome
678 sequencing. *PLoS Gen.* **5**.
679 Langham, G.M. 2004. Specialized avian predators repeatedly attack novel color morphs of
680 Heliconius butterflies. *Evolution* **58:** 2783-2787.
681 Le Poul, Y., Whibley, A., Chouteau, M., Prunier, F., Llaurens, V.Joron, M. 2014. Evolution
682 of dominance mechanisms at a butterfly mimicry supergene. . *Nat. Commun.* **5**.
683 Mallet, J. 1989. The genetics of warning colour in Peruvian hybrid zones od *Heliconius erato*
684 and *H. melpomene*. *Proc. R. Soc. B-Biol. Sci.* **236:** 163-185.
685 Mallet, J.Gilbert, L.E. 1995. Why Are There So Many Mimicry Rings - Correlations between
686 Habitat, Behavior and Mimicry in Heliconius Butterflies. *Biol. J. Linn. Soc.* **55:** 159-
687 180.
688 Mallet, J., Beltran, M., Neukirchen, W.Linares, M. 2007. Natural hybridization in heliconiine
689 butterflies: the species boundary as a continuum. *BMC Evol. Biol.* **7**.
690 Mallet, J. 2008. Hybridization, ecological races and the nature of species: empirical evidence
691 for the ease of speciation. *Philos. Trans. R. Soc. B-Biol. Sci.* **363:** 2971-2986.
692 Mallet, J. 2009. Rapid speciation, hybridization and adaptative radiation in the *Heliconius*
693 *melpomene* group. In: butlin RK, Bridle JR, Schluter D (eds) speciation and patterns
694 of diversity., Cambridge University Press, Cambridge**:** 177-194.
695 Mallet, J. 2010. Shift happens! Shifting balance and the evolution of diversity in warning
696 colour and mimicry. *Ecol. Entomol.* **35:** 90-104.
697 Martin, A., McCulloch, K.J., Patel, N.H., Briscoe, A.D., Gilbert, L.E.Reed, R.D. Multiple
698 recent co-options of Optix associated with novel traits in adaptive butterfly wing
699 radiations. *Evodevo* **5**.
700 Martin, A., Papa, R., Nadeau, N.J., Hill, R.I., Counterman, B.A., Halder, G., et al. 2012.
701 Diversification of complex butterfly wing patterns by repeated regulatory evolution of
702 a Wnt ligand. *Proceedings of the National Academy of Sciences* **109:** 12632.
703 Martin, S.H., Dasmahapatra, K.K., Nadeau, N.J., Salazar, C., Walters, J.R., Simpson, F., et al.
704 2013. Genome-wide evidence for speciation with gene flow in *Heliconius* butterflies.
705 *Genome Res.* **23:** 1817-1828.
706 Mavarez, J., Salazar, C.A., Bermingham, E., Salcedo, C., Jiggins, C.D.Linares, M. 2006.
707 Speciation by hybridization in *Heliconius* butterflies. *Nature* **441:** 868-871.
708 Mavarez, J.Linares, M. 2008. Homoploid hybrid speciation in animals. *Mol. Ecol.* **17:** 4181-
709 4185.
710 Mayr, E. 1963. *Animal Species and Evolution*. (Cambridge, MA: Harvard University Press).
711 Meier, J.I., Marques, D.A., Mwaiko, S., Wagner, C.E., Excoffier, L.Seehausen, O. 2017.
712 Ancient hybridization fuels rapid cichlid fish adaptive radiations. *Nat. Commun.* **8:**
713 14363.
714 Mérot, C., Mavarez, J., Evin, A., Dasmahapatra, K.K., Mallet, J., Lamas, G., et al. 2013.
715 Genetic differentiation without mimicry shift in a pair of hybridizing Heliconius
716 species (Lepidoptera: Nymphalidae). *Biol. J. Linn. Soc.* **109:** 830-847.

Mérot, C., Frérot, B., Leppik, E.Joron, M. 2015. Beyond magic traits: Multimodal mating cues in *Heliconius* butterflies. . *Evolution* **69:** 2891-2904.
Mérot, C., Poul, Y.L., Théry, M.Joron, M. 2016. Refining mimicry: phenotypic variation tracks the local optimum. *J. Anim. Ecol.* **85**.
Merrill, R., Dasmahapatra, K., Davey, J., Dell'Aglio, D., Hanly, J., Huber, B., et al. 2015. The diversification of Heliconius butterflies: what have we learned in 150 years? *J. Evol. Biol.* **28:** 1417-1438.
Merrill, R.M., Schooten, B.V., Scott, J.A.Jiggins, C.D. 2010. Pervasive genetic associations between traits causing reproductive isolation in Heliconius butterflies. *Proc. R. Soc. B-Biol. Sci.*
Merrill, R.M., Wallbank, R.W.R., Bull, V., Salazar, P.C.A., Mallet, J., Stevens, M., et al. 2012. Disruptive ecological selection on a mating cue. *Proc. R. Soc. B-Biol. Sci.* **279:** 4907-4913.
Merrill, R.M., Rastas, P., Melo, M.-C., Martin, S.H., Barker, S., Davey, J., et al. 2018. Genetic dissection of assortative mating behavior. *bioRxiv***:** 282301.
Mitteroecker, P.Bookstein, F. 2011. Linear discrimination, ordination, and the visualization of selection gradients in modern morphometrics. *Evol. Biol.* **38:** 100-114.
Müller, F. 1879. *Ituna* and *Thyridia*: A remarkable case of mimicry in butterflies. *Transactions of the entomological society. London.*
Naisbit, R.E., Jiggins, C.D.Mallet, J. 2003. Mimicry: developmental genes that contribute to speciation. *Evol. Dev.* **5:** 269-280.
Navarro, N.Klingenberg, C.P. 2007. Genetic architecture of the mandible shape: Insights from fine mapping QTLs in a heterogeneous stock of mice. *J. Morphol.* **268:** 1111-1111.
Nolte, A.W., Freyhof, J., Stemshorn, K.C.Tautz, D. 2005. An invasive lineage of sculpins, *Cottus* sp (Pisces, Teleostei) in the Rhine with new habitat adaptations has originated from hybridization between old phylogeographic groups. *Proc. R. Soc. B-Biol. Sci.* **272:** 2379-2387.
Pardo-Diaz, C., Salazar, C., Baxter, S.W., Merot, C., Figueiredo-Ready, W., Joron, M., et al. 2012. Adaptive Introgression across Species Boundaries in *Heliconius* Butterflies. *Plos Genetics* **8:** 13.
Pardo-Diaz C., Salazar C., Baxter S., Mérot C., Figueiredo-Ready W., Joron M., et al. 2012. Adaptive Introgression across Species Boundaries in *Heliconius* Butterflies. *PLoS Gen.* **8**.
Parsons, K.J., Son, Y.H.Albertson, R.C. 2011. Hybridization Promotes Evolvability in African Cichlids: Connections Between Transgressive Segregation and Phenotypic Integration. *Evol. Biol.* **38:** 306-315.
Pereira, R.J., Barreto, F.S.Burton, R.S. 2014. Ecological novelty by hybridization: experimental evidence for increased thermal tolerance by transgressive segregation in *Tigriopus californicus*. *Evolution* **68:** 204-215.
Pitchers, W.R., Nye, J., Márquez, E.J., Kowalski, A., Dworkin, I.Houle, D. 2017. The power of a multivariate approach to genome-wide association studies: an example with Drosophila melanogaster wing shape. *bioRxiv*.
R Core Team 2014. R: A language and environment for statistical computing. R Foundation for Statistical Computing, Vienna, Austria. URL http://www.R-project.org/.
Renaud, S., Alibert, P.Auffray, J.C. 2009. Mandible shape in hybrid mice. *Naturwissenschaften* **96:** 1043-1050.
Renaud, S., Alibert, P.Auffray, J.C. 2012. Modularity as a source of new morphological variation in the mandible of hybrid mice. *BMC Evol. Biol.* **12**.
Renaud, S., Alibert, P.Auffray, J.-C. 2017. Impact of Hybridization on Shape, Variation and Covariation of the Mouse Molar. *Evol. Biol.* **44:** 69-81.

767 Rieseberg, L.H., Archer, M.A.Wayne, R.K. 1999. Transgressive segregation, adaptation and
768 speciation. *Heredity* **83:** 363-372.
769 Rieseberg, L.H., Widmer, A., Arntz, A.M.Burke, J.M. 2003. The genetic architecture
770 necessary for transgressive segregation is common in both natural and domesticated
771 populations. *Philos. Trans. R. Soc. B-Biol. Sci.* **358:** 1141-1147.
772 Rohlf, F. 2010. TpsDig, ver. 2. 16. *Department of Ecology and Evolution, State University*
773 *New York at Stony Brook, New York*.
774 Selz, O.M., Lucek, K., Young, K.A.Seehausen, O. 2014. Relaxed trait covariance in
775 interspecific cichlid hybrids predicts morphological diversity in adaptive radiations. .
776 *J. Evol. Biol.* **27 (1):** 11-24.
777 Servedio, M.R.Noor, M.A.F. 2003. The role of reinforcement in speciation: Theory and data.
778 *Annu. Rev. Ecol., Evol. Syst.* **34:** 339-364.
779 Shivaprasad, P.V., Dunn, R.M., Santos, B., Bassett, A.Baulcombe, D.C. 2012. Extraordinary
780 transgressive phenotypes of hybrid tomato are influenced by epigenetics and small
781 silencing RNAs. *EMBO J.* **31:** 257-266.
782 Smadja, C.Butlin, R. 2006. Speciation - A new role for reinforcement. *Heredity* **96:** 422-423.
783 Srygley, R.B. 1999. Locomotor mimicry in Heliconius butterflies: contrast analyses of flight
784 morphology and kinematics. *Philos. Trans. R. Soc. B-Biol. Sci.* **354:** 203-214.
785 Stelkens, R.Seehausen, O. 2009. Genetic Distance between Species Predicts Novel Trait
786 Expression in Their Hybrids. *Evolution* **63:** 884-897.
787 Stelkens, R.B., Schmid, C., Selz, O.Seehausen, O. 2009. Phenotypic novelty in experimental
788 hybrids is predicted by the genetic distance between species of cichlid fish. *BMC Evol.*
789 *Biol.* **9**.
790 Stelkens, R.B., Brockhurst, M.A., Hurst, G.D.D.Greig, D. 2014. Hybridization facilitates
791 evolutionary rescue. *Evolutionary Applications* **7:** 1209-1217.
792 Stemshorn, K.C., Reed, F.A., Nolte, A.W.Tautz, D. 2011. Rapid formation of distinct hybrid
793 lineages after secondary contact of two fish species (Cottus sp.). *Mol. Ecol.* **20:** 1475-
794 1491.
795 Turner, J.R.G. 1977. Butterfly mimicry - the genetical evolution of an adaptation. . *Evol. Biol.*
796 **10:** 163-206.
797 Wallbank, R.W.R., Baxter, S.W., Pardo-Diaz, C., Hanly, J.J., Martin, S.H., Mallet, J., et al.
798 2016. Evolutionary Novelty in a Butterfly Wing Pattern through Enhancer Shuffling.
799 *PLoS Biol.* **14:** e1002353.
800 Wiens, J.J., Engstrom, T.N.Chippindale, P.T. 2006. Rapid diversification, incomplete
801 isolation, and the "speciation clock" in North American salamanders (Genus
802 plethodon): Testing the hybrid swarm hypothesis of rapid radiation. *Evolution* **60:**
803 2585-2603.
804 Yakimowski, S.B.Rieseberg, L.H. 2014. The role of homoploid hybridization in evolution: A
805 century of studies synthesizing genetics and ecology. *Am. J. Bot.* **101:** 1247-1258.
806 Zelditch, M.L., Swiderski, D.L., Sheets, H.D.Fink, W.L., eds. 2004. *Geometric*
807 *Morphometrics for Biologists*. A Primer. Elsevier Academic Press, San Diego.
808 Zimmerman, E., Palsson, A.Gibson, G. 2000. Quantitative trait loci affecting components of
809 wing shape in Drosophila melanogaster. *Genetics* **155:** 671-683.
810
811

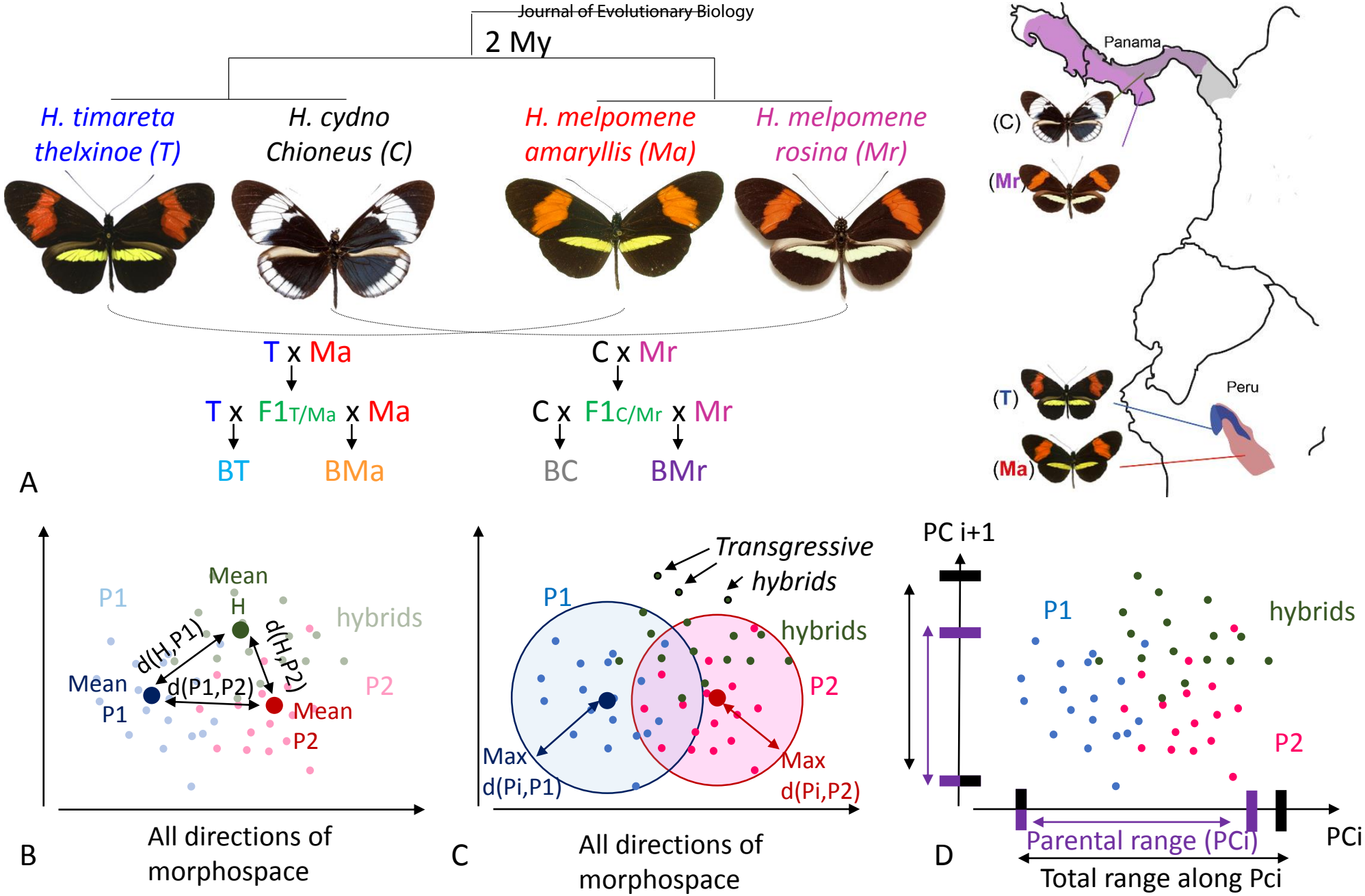
2 My
H. timareta thelxinoe (T)
H. cydno Chioneus (C)
H. melpomene amaryllis (Ma)
H. melpomene rosina (Mr)
T x Ma
C x Mr
T x F1T/Ma x Ma
C x F1C/Mr x Mr
BT
BMa
BC
BMr
A
Panama
(C)
(Mr)
Peru
(T)
(Ma)
Mean H
P1
hybrids
P2
d(H,P1)
d(H,P2)
d(P1,P2)
Mean P1
Mean P2
B
All directions of morphospace
Transgressive hybrids
Max d(Pi,P1)
Max d(Pi,P2)
C
All directions of morphospace
PC i+1
PCi
Parental range (PCi)
Total range along Pci
D

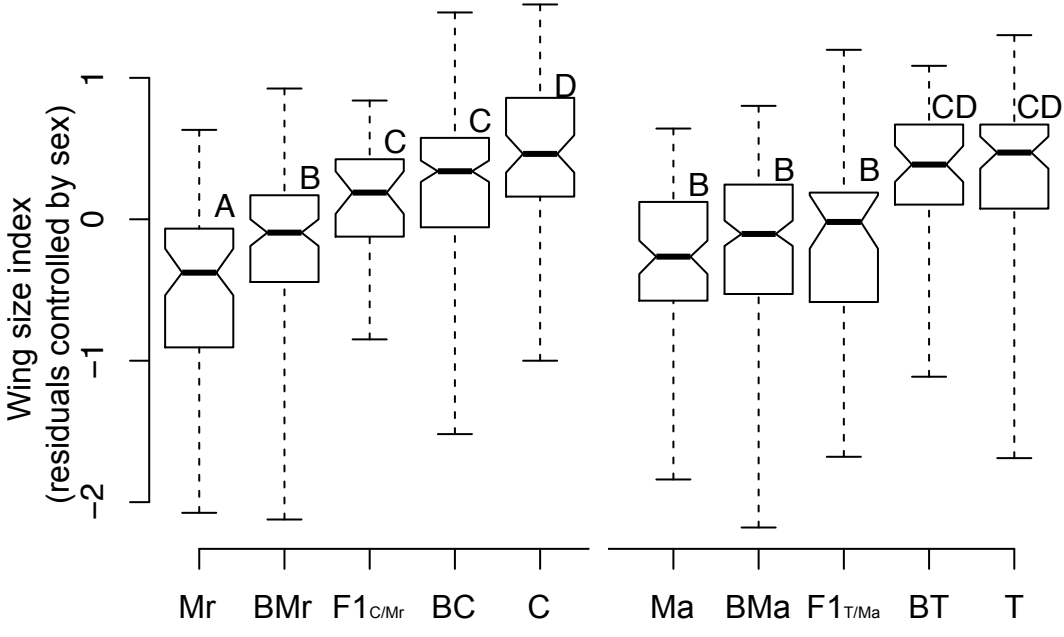
Wing size index
(residuals controlled by sex)
−2
−1
0
1
A
B
C
C
D
B
B
B
CD
CD
Mr
BMr
F1C/Mr
BC
C
Ma
BMa
F1T/Ma
BT
T

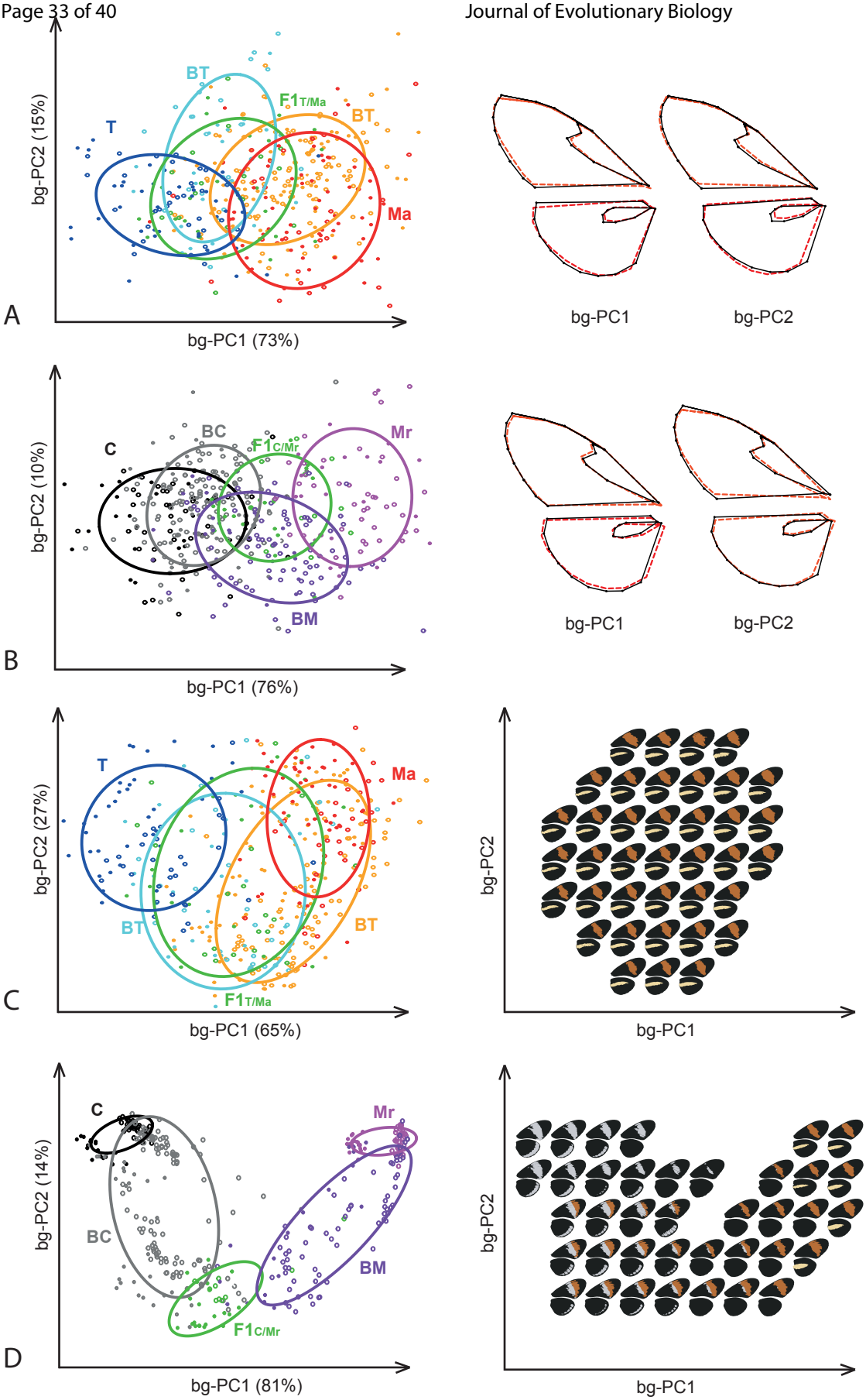
A
BT
F1T/Ma
BT
T
Ma
bg-PC2 (15%)
bg-PC1 (73%)
bg-PC1
bg-PC2
B
BC
F1C/Mr
Mr
C
BM
bg-PC2 (10%)
bg-PC1 (76%)
bg-PC1
bg-PC2
C
T
Ma
BT
BT
F1T/Ma
bg-PC2 (27%)
bg-PC1 (65%)
bg-PC2
bg-PC1
D
C
Mr
BC
BM
F1C/Mr
bg-PC2 (14%)
bg-PC1 (81%)
bg-PC2
bg-PC1

Supplementary materials

Hybridization and transgressive exploration of wing morphology in *Heliconius* butterflies

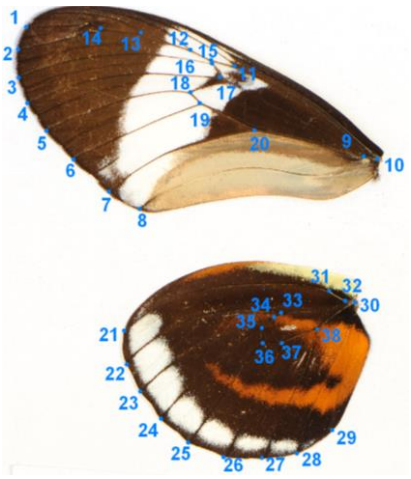

Figure S1. Landmarks used to describe wing shape

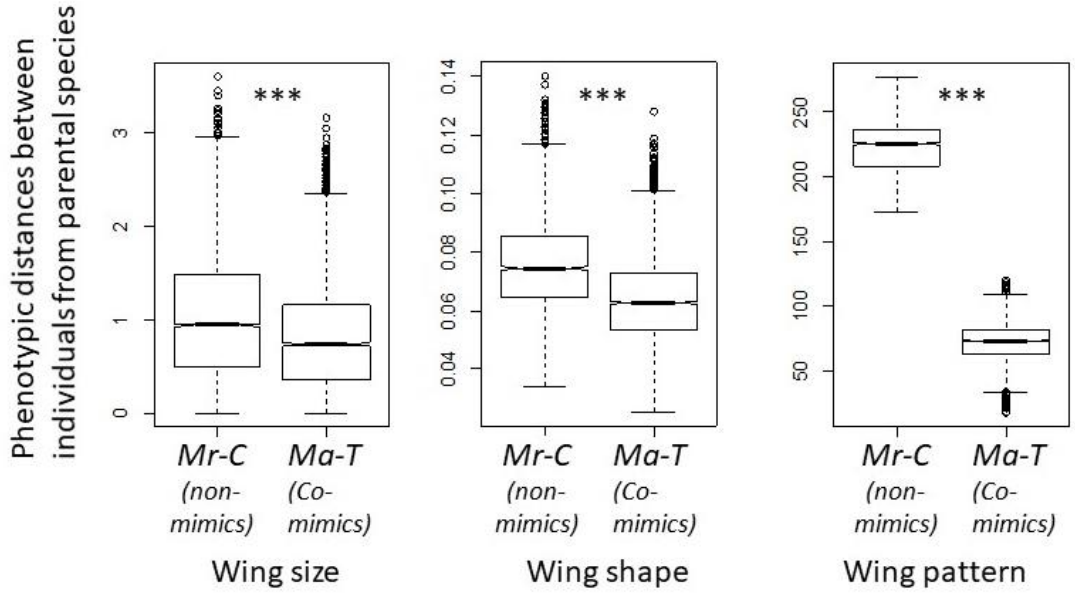

Figure S1. Phenotypic distances between parental distances
Distribution of all pairwise distances between individuals belonging to each parental species.

Table S1. Shape and pattern variation between parental species

	ANOVA/MANOVA		Mean of individual distances			Mahalanobis distances	
	co-mimics *Ma-T*	non-mimics *Mr-C*	co-mimics *Ma-T*	non-mimics *Mr-C*	*ratio*	co-mimics Ma-T	non-mimics Mr-C
size	$F_{1,156}$=41, P<0.001	$F_{1,129}$=90, P<0.001	0.8	1.05	1.3		
shape	$F_{14,143}$=32, Pillai=0.76 P<0.001	$F_{14,116}$=62, Pillai=0.88 P<0.001	0.063	0.076	1.2	11.1	28.8
pattern	$F_{10,139}$=80, Pillai=0.85 P<0.001	$F_{10,99}$=3734, Pillai=0.99 P<0.001	71.9	224.1	3.1	28.7	437

Table S2. Shape and pattern variation between hybrids and parents

LDA(CV) indicates the cross-validation rate when doing a linear discriminant analysis between each hybrid group and each parents

		SHAPE				PATTERN				
		LDA (CV)		MANOVA			LDA (CV)		MANOVA	
		Ma	T	Ma	T		Ma	T	Ma	T
FW	BT	93%	77%	$F_{1,20}$=16.5; p<0.001	$F_{1,20}$=5.4; p<0.001	FW	87%	81%	$F_{1,20}$=10.02; p<0.001	$F_{1,20}$=6.4; p<0.001
	BMa	79%	95%	$F_{1,20}$=9.0; p<0.001	$F_{1,20}$=26.8; p<0.001		77%	98%	$F_{1,20}$=6.8; p<0.001	$F_{1,20}$=55.8; p<0.001
	$F1_{T/Ma}$	93%	83%	$F_{1,20}$=11.4; p<0.001	$F_{1,20}$=7.1; p<0.001		82%	85%	$F_{1,20}$=6.5; p<0.001	$F_{1,20}$=10.1; p<0.001
		Mr	C	Mr	C		Mr	C	Mr	C
FW	BC	89%	78%	$F_{1,20}$=19.7; p<0.001	$F_{1,20}$=7.7; p<0.001	FW	98%	91%	$F_{1,20}$=257.6; p<0.001	$F_{1,20}$=17.7; p<0.001
	BMr	87%	89%	$F_{1,20}$=11.3; p<0.001	$F_{1,20}$=17.8; p<0.001		88%	100%	$F_{1,20}$=14.4; p<0.001	$F_{1,20}$=2071; p<0.001
	$F1_{C/Mr}$	84%	85%	$F_{1,20}$=7.7; p<0.001	$F_{1,20}$=6.5; p<0.001		99%	100%	$F_{1,20}$=248.9; p<0.001	$F_{1,20}$=1134; p<0.001
		Ma	T	Ma	T		Ma	T	Ma	T
HW	BT	88%	75%	$F_{1,20}$=11.6; p<0.001	$F_{1,20}$=4.5; p<0.001	HW	84%	87%	$F_{1,20}$=104; p<0.001	$F_{1,20}$=9.9; p<0.001
	BMa	74%	93%	$F_{1,20}$=6.6; p<0.001	$F_{1,20}$=22.1; p<0.001		71%	95%	$F_{1,20}$=4.3; p<0.001	$F_{1,20}$=37.5; p<0.001
	$F1_{T/Ma}$	79%	79%	$F_{1,20}$=6.2; p<0.001	$F_{1,20}$=5.9; p<0.001		75%	81%	$F_{1,20}$=3.8; p<0.001	$F_{1,20}$=7.3; p<0.001
		Mr	C	Mr	C		Mr	C	Mr	C
HW	BC	96%	82%	$F_{1,20}$=42.2; p<0.001	$F_{1,20}$=9.1; p<0.001	HW	100%	83%	$F_{1,20}$=3994; p<0.001	$F_{1,20}$=10.1; p<0.001
	BMr	82%	93%	$F_{1,20}$=12.3; p<0.001	$F_{1,20}$=24.5; p<0.001		90%	100%	$F_{1,20}$=23.5; p<0.001	$F_{1,20}$=279; p<0.001
	$F1_{C/Mr}$	86%	91%	$F_{1,20}$=7.5; p<0.001	$F_{1,20}$=14.2; p<0.001		100%	90%	$F_{1,20}$=888; p<0.001	$F_{1,20}$=22.4; p<0.001

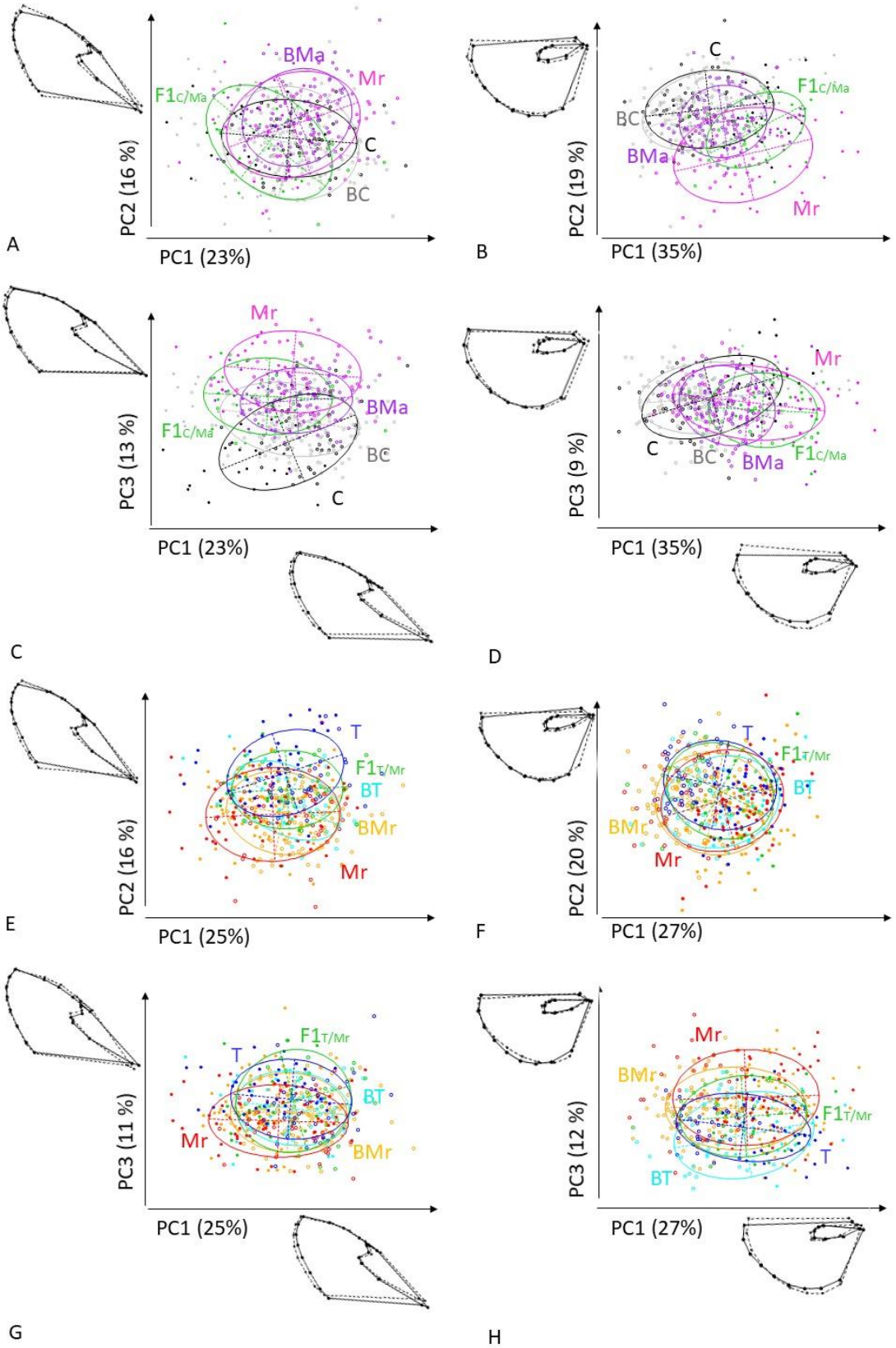

Figure S3. PCA on forewing and hindwing shape

PCA on wing shape for parents and hybrids between *H. cydno chioneus* and *H. melpomene rosina* on forewing pattern **(A, C)** and the hindwing pattern **(B, D)**, between *H. timareta thelxinoe* and *H. melpomene* on forewing pattern **(E, G)** and the hindwing pattern **(F, H).** Open circles represent females and filled dots represent males. Shape variation is illustrated next to each axis, where broken lines represent minimum negative values of the axis, and full lines represent maximum values.

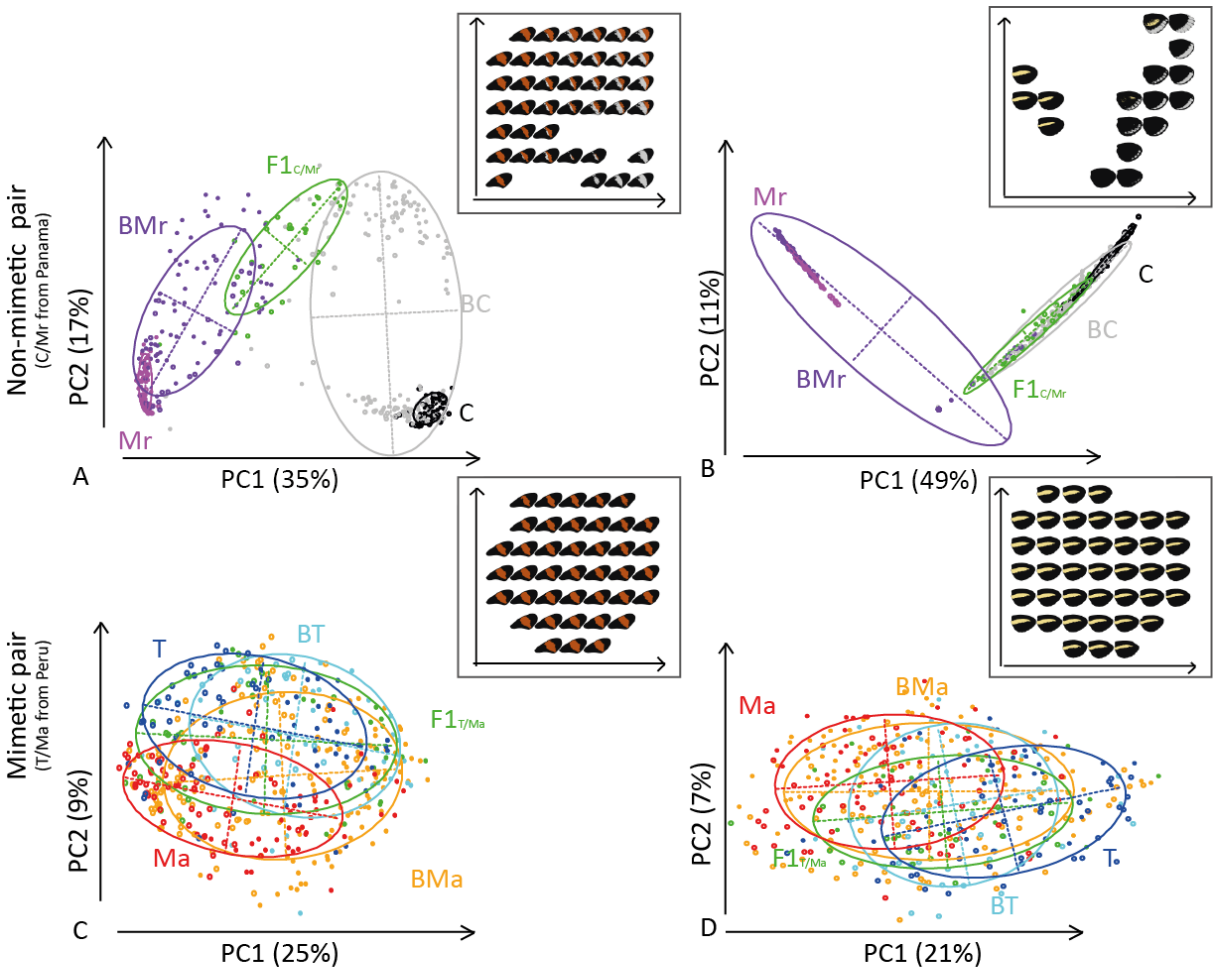

Figure S4. Variation of hybrid wing pattern.
PCA on wing pattern for parents and hybrids between *H. cydno chioneus* and *H. melpomene rosina* on forewing pattern **(A)** and the hindwing pattern **(B)**, between *H. timareta thelxinoe* and *H. melpomene* on forewing pattern **(C)** and the hindwing pattern **(D).** The insert display morphological variation in each PCA space. Open circles represent females and filled dots represent males.

Table S3. Transgression strength along each PC direction

%var stands for the variation explained by the given PC, Ts Pci is the difference between total range and parental range, expressed as a fraction of parental range along each PC.

Ts is the global index and Max the maximum Ts Pci.

		BMa		F1T/A		BT		BMr		F1C/Mr		BC	
		Ts Pci	%var	Ts Pci	%var	Ts Pci	%var	Ts Pci	%var	Ts Pci	%var	Ts Pci	%var
shape	PC1	0.000	19%	0.000	20%	0.000	21%	0.000	17%	0.000	18%	0.000	21%
	PC2	**0.140**	15%	0.000	14%	0.000	15%	0.000	15%	0.000	16%	**0.130**	15%
	PC3	**0.070**	9%	**0.014**	10%	0.000	10%	0.000	13%	0.000	14%	**0.031**	11%
	PC4	**0.150**	7%	0.000	8%	0.000	7%	0.000	8%	**0.092**	8%	**0.044**	7%
	PC5	**0.049**	6%	0.000	6%	**0.061**	6%	**0.094**	6%	0.000	7%	**0.210**	6%
	PC6	0.000	5%	0.000	5%	0.000	5%	**0.038**	5%	**0.320**	5%	**0.044**	5%
	PC7	0.000	5%	**0.071**	5%	**0.080**	5%	**0.280**	4%	0.000	4%	**0.150**	4%
	PC8	**0.190**	4%	**0.016**	4%	0.000	3%	**0.380**	3%	0.000	3%	**0.190**	3%
	PC9	**0.073**	3%	0.000	3%	**0.078**	3%	**0.096**	3%	0.000	3%	**0.220**	3%
	PC10	**0.080**	3%	0.000	3%	0.000	3%	0.000	3%	0.000	2%	**0.170**	2%
	PC11	**0.140**	2%	**0.079**	2%	0.000	2%	**0.200**	2%	0.000	2%	0.000	2%
	PC12	**0.035**	2%	0.000	2%	0.000	2%	**0.068**	2%	**0.029**	2%	**0.066**	2%
	PC13	**0.067**	2%	0.000	2%	0.000	2%	**0.004**	2%	0.000	2%	**0.094**	2%
	PC14	0.000	2%	0.000	2%	0.000	2%	0.000	2%			0.000	2%
	Ts	**0.069**		**0.008**		**0.012**		**0.046**		**0.027**		**0.077**	
	Max	**0.190**		**0.079**		**0.080**		**0.380**		**0.320**		**0.220**	
pattern	PC1	**0.041**	53%	0.000	52%	0.000	53%	**0.014**	57%	0.000	65%	0.000	64%
	PC2	**0.440**	9%	**0.160**	9%	**0.037**	9%	**2.900**	12%	**2.900**	13%	**3.300**	11%
	PC3	**0.085**	6%	**0.047**	7%	0.000	7%	**1.400**	7%	**0.290**	4%	**0.520**	3%
	PC4	0.000	4%	0.000	4%	0.000	4%	**0.550**	3%	0.000	3%	**0.550**	3%
	PC5	0.000	3%	**0.045**	3%	0.000	3%	**0.038**	3%	**0.260**	2%	**0.410**	2%
	PC6	**0.160**	2%	**0.019**	3%	0.000	2%	**0.410**	2%	**0.140**	1%	**0.440**	2%
	PC7	**0.087**	2%	**0.055**	2%	**0.033**	2%	0.000	1%	**0.240**	1%	**0.630**	1%
	PC8	**0.310**	2%	**0.017**	2%	0.000	2%	**0.830**	1%	**0.280**	1%	**0.280**	1%
	PC9	**0.170**	2%	0.000	2%	**0.050**	2%	**0.170**	1%			**0.900**	1%
	PC10	**0.086**	1%	**0.250**	1%	0.000	1%						
	PC11	**0.082**	1%	0.000	1%	**0.083**	1%						
	PC12	**0.150**	1%										
	PC13	**0.210**	1%										
	Ts	**0.099**		**0.028**		**0.006**		**0.566**		**0.446**		**0.489**	
	Max	**0.440**		**0.250**		**0.083**		**2.900**		**2.900**		**3.300**	

Table S4. Mean transgression controlled by the ratio of parental distances

Since the index *Tm* is standardized by the distance between parents, this might artificially bias index values towards higher values when species are more similar. For instance, we noted that, in the null model, simulated hybrids have a higher transgression of the mean in the co-mimetic pair than in the non-mimetic pair. Therefore, we also compared the transgression value when correcting from the ratio of parental distances (Table S1).

	Tm in non-mimetic hybrids		Tm in mimetic hybrids		Tm in mimetic hybrids Controlled by the ratio of parental distances
Pattern (parental ratio = 3.1)	BMr	0.22	Bma	0.41	0.13
	F1CMr	0.48	F1TMa	0.27	0.09
	BC	0.21	BT	0.42	0.14
Shape (parental ratio = 1.2)	BMr	**0.16**	Bma	0.27	**0.23**
	F1CMr	0.22	F1TMa	0.2	0.17
	BC	**0.16**	BT	0.44	**0.37**